

## **EXPLORING THE EFFECT OF BIOACTIVE COMPOUNDS FROM ETHYL ACETATE FRACTION OF *HYPTIS VERTICILLATA* JACQ LEAF AS POTENTIAL ANTI-DIABETIC AGENTS: DFT, MOLECULAR DOCKING AND PHARMACOKINETIC STUDIES**

**Ukam, Catherine Ironya-Ogar<sup>a\*</sup>, Ogar, Blessing Thomas<sup>a</sup>, Egbung, Josephine Eneji<sup>d</sup>, Henry O. Edet<sup>b,c</sup>, Chume, Sandra<sup>a</sup> O., Abuo Patrick A<sup>a</sup>, Ibiam Okoro K<sup>a</sup>, Akpan E. Monday<sup>a</sup>, Ekundayo Micheal Temitope<sup>a</sup>, Atangwho, Item Justin<sup>a</sup> and Egbung, Godwin Eneji<sup>a</sup>**

<sup>a</sup>Department of Biochemistry, Faculty of Basic Medical Sciences, University of Calabar Nigeria

<sup>b</sup>Computational and Bio-Simulation Research Group, University of Calabar, Calabar, Nigeria

<sup>c</sup>Department of Biochemistry, Faculty of Physical Sciences, University of Cross River State, Nigeria

<sup>a</sup>Department of Human Nutrition and Dietetics, Faculty of Basic Medical Sciences, University of Calabar Nigeria

**Corresponding author's email:** [ironyacathy.u@gmail.com](mailto:ironyacathy.u@gmail.com); [ironyaogar@yahoo.com](mailto:ironyaogar@yahoo.com);  
[drironya@unical.edu.ng](mailto:drironya@unical.edu.ng)

---

### **Abstract**

The present study explored the antidiabetic efficacy of the ethyl-acetate fraction of the *H. verticillata* leaf using experimental and theoretical simulations including molecular docking. Natural bond order analysis revealed intense molecular interactions of identified bioactive compounds in order of increasing strength to include 2-Chloropropionic acid (289.56 kcal/mol) > 1,4-Eicosadiene (91.45 kcal/mol) > Naphthalene (89.23 kcal/mol) > 2-amino-1-phenylethanol (57.22 kcal/mol) > Benzoic acid (50.23 kcal/mol). Results of the molecular docking showed that the bioactive compounds in *H. verticillata* exhibited promising binding affinities, showing superior inhibitory effects on  $\alpha$ -amylase and  $\alpha$ -glucosidase compared to Miglitol and Acarbose. Pharmacokinetic assessments revealed favourable gastrointestinal absorption, oral bioavailability, and aqueous solubility of the bioactive compounds. Toxicity studies indicated the compounds' inertness to mutagenicity and cytotoxicity, further supporting their potential as safe anti-diabetic agents. Collectively, these findings present compelling evidence for the pharmacological viability of *H. verticillata* leaf extract as a highly promising anti-diabetic treatment option.

**Keywords:** DFT, *In-silico* molecular docking, *H. verticillata* Jacq, ADMET,

## 1.0 Introduction

Diabetes Mellitus (DM) is a chronic metabolic disorder characterized by hyperglycaemia arising from deficiency in insulin secretion, aberrant insulin function or both. As a result of insufficient secretion of insulin by the pancreas or the non-response of the body cells to insulin production which is crucial for normal body metabolism [1]. Particularly, Type 2 diabetes mellitus (T2DM) is among the most prevalent forms of the disease diagnosed globally and accounts for 90% of instances of diabetes reported, with middle-aged people in low- and middle-income nations being the main victims [2]. The most compelling evidence indicating an age-related increase in diabetes prevalence points to the fact that approximately 25% of individuals over the ages of 65 are afflicted with diabetes [1]. Consequently, T2DM develops as a result of ineffective response of the body cells to insulin production and it is typically characterized by insulin resistance which implies the inability of the target organs to respond naturally to the action of insulin [3]. This leads to the partial suppression of glucose output by the liver accompanied by impaired insulin-mediated glucose uptake in the periphery (skeletal muscle and adipose) leading to increased need for insulin [4]. When insulin requirements are not met by increased insulin level, hyperglycaemia occurs. Severe hyperglycaemia in diabetic patients can lead to organ dysfunction, accompanied by micro-vascular and macro-vascular complications resulting in increased cardiovascular problem [5]. The rise in global diabetes cases can be attributed to unhealthy lifestyles, including physical inactivity and alcohol consumption. Insulin resistance is also associated with other conditions such as central obesity, hypertension, metabolic syndrome and polycystic ovary syndrome

(PCOS) [6]. In addition to the overall composition of the body fat, distribution of adipose tissue plays a crucial role in visceral depots contributing significantly to insulin resistance. Ongoing research are actively exploring the mechanisms linking the accumulation and anatomical distribution of adipose tissue to the development of insulin resistance. Nevertheless, injectables and oral anti-diabetic medications have been prescribed for use in the treatment of the prevalent type 2 diabetes. These drugs primarily function by inhibiting key metallo-enzymes, including  $\alpha$ - amylase and the  $\alpha$ -glucosidase. The pancreatic  $\alpha$ - amylase (EC 3.2.1.1) and the  $\alpha$ -glucosidase (EC 3.2.1.20) are responsible for the digestion of starch at different stages [7]. These medications reduce the rate of carbohydrate digestion, thereby preventing sudden spikes in glucose levels thereby, effectively managing blood glucose levels in diabetic patients [8].

In the search for improved anti-diabetic compounds, phytochemicals have demonstrated significant antihyperglycaemic effects with little or no side effects [8]. Oral anti-diabetic agents in form of herbs have been widely explored in the prevention and treatment of diabetes taking advantage of the floral biodiversity of potential anti-diabetic plants [9]. Plants from the *Hyptis* genus have shown promising medicinal potentials. For instance, Picking et al [10] reported the anti-miotic, anti-proliferative, cytotoxic, antioxidant, anti-inflammatory, anti-bacterial, anti-fungal; anti-viral and hepatoprotective properties of *H. verticillata* jacq. Ogar et al [5] and Vanessa et al [11] reported anti-diabetic potential of plant species belonging to *H.* genus. The ethanolic and petroleum extract of *H. suaveolens* plants had comparable effects as the standard insulin, by reducing blood glucose level thereby

simulating peripheral glucose utilization. Its chloroform extracts exhibited antioxidant potential in diabetic rat models and inhibitory potential on salivary  $\alpha$ -amylase. The ethanolic extract of *H. verticillata jacq* administered to streptozotocin-induced diabetic rats decreased their HbA1c and fasting blood glucose level. Lianza et al [12] reported the  $\alpha$ -glucosidase activity of *H. Monticola* flower and the leaves of *Lantana trifolia* and *Lippia origanoides*. Results showed the inhibitory potentials of the extracts on  $\alpha$ -glucosidase enzyme. Picking et al., [13] investigated the antioxidant properties using the (DPPH assay) and chemical characterization (LC-MS) of *Hyptisverticillata jacq* plant extracts and its inhibitory effect on the activities of cytochrome P450, enzyme (CYPS 1A1, 1A2, 1B1, 3A4 and 2D6), the dried plant ethanol extract showed the inhibition of the enzyme CYPS 1A1, 1A2, 1B1, 3A4 against the fresh plant extract. Although other works have been carried out on *H. verticillata jacq*, its clinical application as an anti-diabetic agent is yet to be fully explored. Therefore, this research was aimed at investigating the anti-diabetic potentials of *H. verticillata* leaf extracts through experimental and theoretical simulations by utilizing in-silico molecular docking protocol and drug-likeness (pharmacokinetic) investigation in order to maximize their therapeutic potentials.

## 2.0 Materials and methods

### 2.1 Preparation of plant extract

Fresh leaves of *H. Verticillata* were rinsed thoroughly in clean tap water and thereafter in distilled water, dried under shade for 14 days, blended into powder and stored in airtight plastic containers. Thereafter, 1220 g of

the powdered leaves was macerated in 98 % ethanol at room temperature for 48 hours. The extract was double filtered using cheese cloth, followed by rotary evaporation to yield 127.9 g of crude extract, which led to a percentage yield of 10.5 %. The extract was then refrigerated at 4 °C pending usage. To obtain the ethyl-acetate fraction, the crude ethanol extract was chromatographically eluted with three different solvents, including n-hexane, acetone and ethyl acetate in a column packed with silica gel. The fractions were collected and evaporated in rotary evaporator at 50 oC to 10 % of its original volume and was further evaporated to paste form in a water bath at 50 oC. The resulting ethyl-acetate fraction was stored in a freezer at 4 oC for further experiments.

## 2.2 Anti-diabetic properties

### 2.2.1 GC-MS scan method

This analysis was performed using 6890 A gas chromatograph coupled to 5973 C inert mass spectrometer (with triple axis detector) and electron impact source (Agilent Technologies) according to an earlier reported method [5].

### 2.3 Estimation of $\alpha$ -glucosidase inhibitory activity

The  $\alpha$ -glucosidase inhibitory activity was assessed by the standard method, with slight modifications. Briefly, 200  $\mu$ L of each extract or acarbose/miglitol at different concentrations were incubated with 500  $\mu$ L of  $\alpha$ -glucosidase solution in 100 mM phosphate buffer (pH 6.8) for 15 minutes. Thereafter, 250  $\mu$ L of  $\rho$ -Nitrophenyl- $\alpha$ -D-glucopyranoside ( $\rho$ NPG) solution was added, and the mixture was further incubated at 37 °C for 20 min. The absorbance of the released  $\rho$ -nitrophenol was measured at 405 nm, and

the inhibitory activity was expressed as a percentage of control without inhibitors.

#### 2.4 Estimation of $\alpha$ -amylase inhibitory activity

The assay system comprised the following components in a total volume of 200  $\mu$ L of each extract or acarbose/miglitol at different concentrations was incubated with 500  $\mu$ L of porcine pancreatic amylase at 37 °C for 20 minutes. An aliquot (250  $\mu$ L) of 1% starch solution was then added to the reaction mixture and incubated at 37 °C for 1 hour. 1mL of DNS colour reagent was then added and boiled for 10 minutes. The absorbance of the resulting mixture was measured at 540 nm, and the inhibitory activity was expressed as a percentage of control without inhibitors.

#### 2.5 Phytochemical analysis

##### 2.5.1 Phytochemical screening

The extract fractions of *H. verticillata* was subjected to qualitative and quantitative phytochemical analysis to identify the phytochemicals present. The extract was used for phytochemical screening as described by Soforowa, (1993) [14]; Trease and Evans, (1996) [15] and Harborne, (1998) [16] respectively.

#### 2.6 Qualitative and Quantitative phytochemical composition of extract fractions of *H. verticillata* leaf

The results of the qualitative and quantitative phytochemical composition of *H. verticillata* (HV) are presented in Table SI. The qualitative analysis indicated the presence of tannins, phenol, reducing sugars and flavonoids in the whole extract and ethyl acetate fraction while alkaloids and saponins were detected only in the whole extract. The highest phenol content was in the ethyl acetate fraction at 60 %. The ethyl acetate

fraction possessed the highest content of flavonoids at 100 %.

#### 2.6.1 In vitro alpha-amylase and alpha glucosidase activity of *H. verticillata* leaf extract and solvent fractions.

The highest  $\alpha$ -amylase inhibition activity was noticed in the ethyl-acetate fraction followed by the whole extract SI fig1 and 2. This order was changed in the  $\alpha$ -glucosidase activity with the highest  $\alpha$ -glucosidase activity observed in the ethyl-acetone fraction.

#### 2.7 Computational details

The computational details of the study were conducted utilizing the Kohn-Sham Density Functional Theory (DFT) to assess the diabetic inhibition potential of the phytochemicals under investigation. Ground state geometry optimizations were carried out using Gaussian 16 software. To ensure stable molecular geometry and computational accuracy, the optimizations were performed in the gas phase employing the Becke's Parameter exchange functional with Lee, Yang, and Parr's gradient correlation (B3LYP) along with the def2svp basis set for lighter atoms. The calculations were conducted within Gauss View 6.0.16 and Gaussian 09 software. The chosen basis set was selected for its ability to provide precise structural properties and account for long-range correlation effects in non-covalent bonds. Frequency optimizations were conducted at the same level of theory to validate the stability of the optimized structures. The absence of imaginary frequencies confirmed the emergence of energetically favourable minima on the potential energy surface of the receptors. Frontier molecular orbitals were also calculated at the same level of theory to provide insights into the electronic properties of the studied compounds. The optimized geometry structures were visualized using

Gauss View 6.0 software. Natural Bond Orbital (NBO) analysis, which elucidates intra and intermolecular charge transfer, was performed using NBO 3.0 software and the results were analysed with Notepad++. For molecular docking studies, the optimized structures were docked with receptor proteins obtained from the Protein Data Bank using

PyRx software. Additionally, the Absorption, Distribution, Metabolism, Excretion (ADME) parameters and toxicity profiles of the compounds were evaluated using SwissADME and ProTox-II tools, respectively, to assess their pharmacokinetic properties and potential adverse effects.

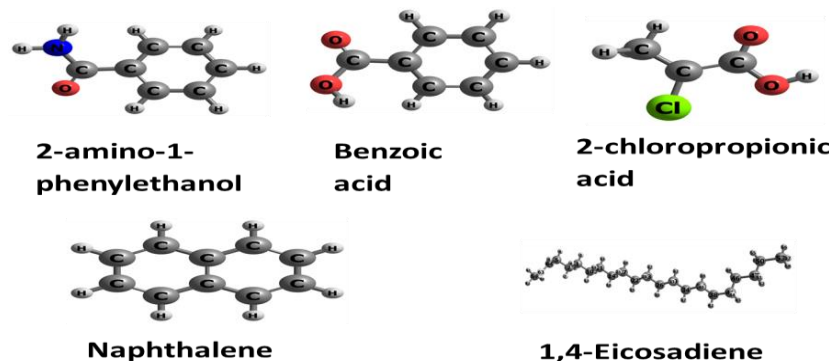


Plate 1: Structure of the bioactive compounds optimized at B3LYP/def2svp basis set

### 3.0 Results and Discussion

#### 3.1 Frontier molecular orbital analysis

The obtained results from the study highlight the electronic and structural properties of the compounds in the ethyl-acetate fraction of *H. verticillata* leaf extract presented on plate 1, shedding light on their potential anti-diabetic activity. Frontier molecular orbital analysis reveals the characteristics of the highest occupied molecular orbital (HOMO) and the lowest unoccupied molecular orbital (LUMO), providing detail knowledge into the compounds' nucleophilic and electrophilic nature, respectively [18]. The energy gap ( $E_g$ ) between the HOMO and LUMO plays a significant role in explaining the ease of electron transfer within the

complexes. A lower energy gap indicates increased polarizability and electron transfer from the HOMO to the LUMO. In this study, compounds like Benzoic acid, 2-amino-1-phenylethanol, 1,4 Eicosadiene, and Naphthalene exhibit higher energy gap values, signifying their stability. On the other hand, 2-Chloropropionic acid displays lower stability due to its decreased energy gap value. Understanding the stability and reactivity of these compounds is essential for assessing their potential as bioactive agents, with respect to the anti-diabetic activity. By examining the energy gap values and electronic properties of the compounds, this study aims to elucidate the specific bioactive components responsible for the observed anti-diabetic effects in the ethyl-acetate fraction of *H. verticillata* extract.

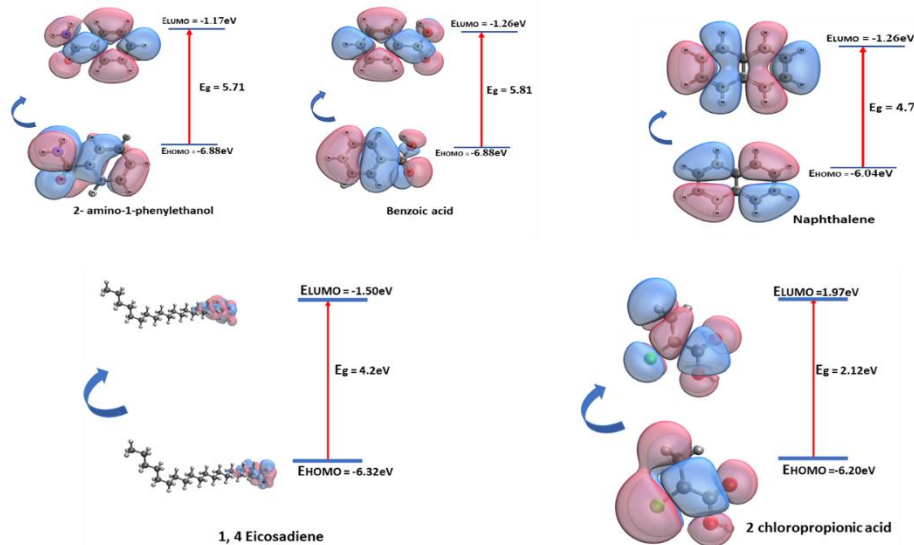


Plate 2: The HOMO-LUMO distribution of the studied bioactive compounds

### 3.2 Global quantum reactivity descriptors

The results obtained from the calculations of various molecular descriptors for the studied bioactive compounds provide significant implications for understanding their properties and potential applications. The calculated values of ionization potential (IP), electron affinity (EA), energy gap (Eg), chemical hardness ( $\eta$ ), and electrophilicity index ( $\omega$ ) offer insights into the stability, reactivity, and biological activity of the compounds. The ionization potential values reflect the compounds' stability and chemical inertness, with higher values indicating greater stability and lower reactivity. This suggests that the compounds may exhibit enhanced drug absorptivity in biological systems. On the other hand, lower ionization energy values signify higher reactivity of the compounds, which can be important for their bioactivity. Notably, compounds like naphthalene, with the lowest ionization potential value of 12.790, would be more prone to undergo chemical reactions and interactions in biological systems [20]. This

increased reactivity suggests that naphthalene may have enhanced drug absorptivity compared to compounds with higher ionization potential values. Therefore, from the obtained results, naphthalene stands out among the studied compounds due to its lower ionization potential value, indicating a higher likelihood of interacting with biological targets and potentially exhibiting pharmacological activity. The energy gap values between the HOMO and LUMO levels (plate 2), provide information on the compounds' reactivity and stability. A larger energy gap indicates higher stability and lower reactivity, while a smaller energy gap suggests potential reactivity and instability. This suggests that compounds with larger energy gaps may be more stable and less reactive (1,4-Eicosadiene > Benzoic acid, > 2-chloropropionic acid > Naphthalene), while those with smaller energy gaps may be more prone to chemical reactions. The chemical hardness values, derived from the energy gap, further characterize the stability and reactivity of the compounds. Higher hardness values indicate greater stability,

while lower values can suggest increased reactivity. Moreover, the electrophilicity index values reveal the compounds' tendencies to interact in biological systems, with higher values indicating efficiency and reactivity.

Thus, the obtained results and calculated values provide valuable information about the electronic properties and reactivity of the studied compounds, shedding light on their potential biological activities and applications.

Table 1: Computed chemical descriptors of the studied bioactive compounds calculated at B3LYP/def2svp

Compounds	Homo (eV)	Lumo(eV)	Eg	IP	EA	- $\mu$ (eV)	H	$\sigma$	$\Omega$
2-amino-1-phenylethanol	-6.889	-1.175	5.7	9.8	1.1	-4.032	2.8	0.17	35.84
			1	9	75		57	4	5
Benzoic acid	- 7.426	-1.613	5.8	7.4	1.6	-4.520	2.9	0.17	45.51
			1	2	1		06	2	5
Naphthalene	-6.044	-1.260	4.7	6.0	1.2	-3.653	2.3	0.20	12.79
			8	4	6		91	9	0
1,4-Eicosadiene	-6.325	-0.055	6.2	6.3	0.5	-3.191	3.1	0.15	1.623
			7	3	5		35	9	
2-chloropropionic acid	-6.203	-1.972	5.2	12.	6.2	-3.587	2.6		24.46
			3	97	0		15	0.19	0
								1	

### 3.3 Natural Bond Orbital (NBO)

The natural bond orbital (NBO) analysis is one of the vital tools which elucidate chemical bonds derived theoretically from the Schrödinger wave function of molecules. It equally accounts for effect of resonance structures molecules. The natural bond order was developed by Weinhold et al [21] and it primarily focuses on the stabilization of molecules via electron density delocalization, charge transfer, inter-hybridization, hyper-conjugative interactions and charge transfer which can be explored by analysing the second order perturbation energy  $E^{(2)}$ . This concept highlights the importance of charge

transfer or intermolecular interactions occurring between the filled and vacant acceptor NBOs. It is employed for investigating intra and inter molecular interactions or conjugative interactions in molecules. Conjugative interactions arise from electron transfer due to electron delocalization from the (occupied) donor NBO to the (Vacant) acceptor NBO. The delocalization of electron density between the bond or lone pair orbital and the unoccupied anti-bonding or Rydberg orbitals conforms to a stabilized donor-acceptor interaction for the donor (i) and acceptor (j) NBO [22]. The magnitude of the donor-

acceptor interaction can be thoroughly explored by utilizing the stabilization energy  $E(2)$ .

$$E^{(2)} = q_i \frac{(F_{ij})^2}{E(i) - E(j)}$$

For each donor NBO (i) and acceptor NBO (j), where  $q_i$  is the orbital occupancy,  $E(i) - E(j)$  are diagonal elements and  $F_{ij}$  is the off diagonal NBO fock matrix element. As shown in table SI 2, the prominent interactions which present were the hyper-conjugative interactions, the Rydberg (RY) and the centre core pair (Cr) where loosely bond interactions occur. For the Benzoic acid moiety, the intra-molecular interactions with the highest stabilization energy of 50.23Kcal/mol and 45.22Kcal/mol were traceable to  $\text{LP}^* - \pi^*$  and  $\text{LP}^* - \sigma$ . Naphthalene recorded the highest perturbation energy 89.23Kcal/mol and 75.26 Kcal/mol generated for the intra-molecular interaction between  $\sigma$  C10 – C21 to  $\text{LP}^*$  H49 and  $\sigma$  C9 – C20 to  $\text{LP}^*$  H49 and  $\sigma$  C9-C20 to  $\pi^*$  C11 - C17 respectively. The donor -interaction with the highest stabilization energy for 1, 4-Eicosadiene are  $\pi^*$  C7- C18 to  $\sigma$  C18 - H53 and  $\sigma$  C15 – C17 to  $\sigma^*$  C14 - H51 with corresponding energy of 156.35Kcal/mol and 90.05Kcal/mol respectively. The highest perturbation energy for 2-chloropropionic were obtained at 289.56Kcal/mol and 224.01 Kcal/mol for the donor-acceptor interactions of  $\sigma$  C15 - H30 to  $\sigma^*$  C14 - H 52 and  $\sigma$  C15 - H30-  $\sigma^*$  C1 - H25 respectively.

### 3.4 Visualization Studies

#### 3.4.1 Non-Covalent Interaction

Non-covalent interaction determines the stability and the nature of both intra and inter-molecular interactions in molecules. Noncovalent interactions include various extents of molecular interactions such as London dispersion forces, dipole-dipole interactions, repulsion forces and hydrogen bond [23]. The reduced density gradient (RDG), second density Hessian Eigen value of the diagonalized Hessian matrix represented by  $(\lambda 2)(r)$  and the electron density  $(p)(r)$  are the significant parameters for evaluating non-covalent interaction. The NCI can be spotted in three dimensional zones where the electron density  $(p)$  and RDG is almost zero.

The plot of (RDG) and the sign  $\lambda 2(r)(p)(r)$  are imperative for the determination of specific regions with non-covalent interaction [24]. The value of the RDG distinctively distinguishes the nature of non-covalent interaction present in complexes as portrayed in plate 3. The non-dimensional reduced gradient analysis (RDG) function can be expressed as The RDG iso-surface is typically expounded on the basis of the three different colours by the paraded by the complexes. The blue region represents neighbouring hydrogen bond, the red region denotes zone portrays zones weak Vander Waal forces and without exceptions the green depicts zones of stearic hindrance [25]. However, the parameters  $\Delta\rho$  and  $\rho$  symbolizes the electronic density gradient and electron density respectively. The green iso-surface portrayed in the 2D plots and the RDG scatter diagram presented in plate 3.

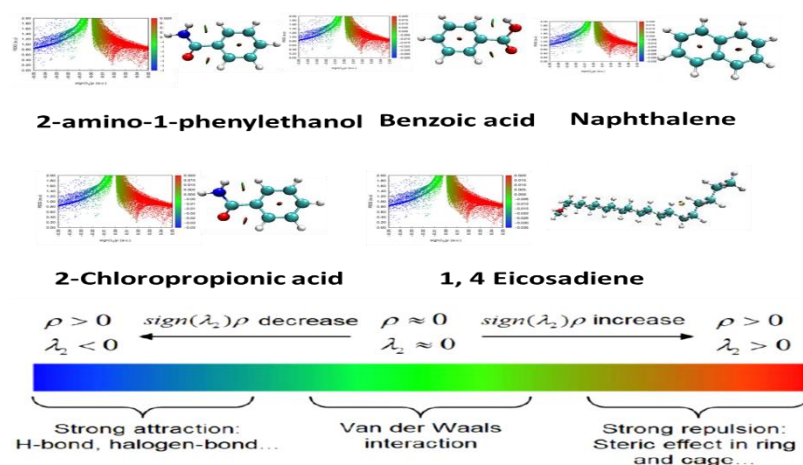


Plate 3: 2D reduced density gradient (RDG) and 3D Isosurface plots of the selected bioactive compounds

### 3.4.2 Topological analysis- quantum theory of atoms-in-molecules (QTAIM) and electron localization function ELF

The study aims to utilize the quantum theory of atoms-in-molecules (QTAIM) within the context of topological studies to investigate the nature and impact of hydrogen bonds and non-covalent interactions on inter-atomic interactions. The framework of QTAIM is recognized for its reliability and suitability for understanding the strength and characteristics of intermolecular bonds, particularly through the analysis of bond critical points (BCP) that connect two atoms. These BCPs play a fundamental role in unravelling the chemical bonding within molecules by exploring various topological parameters such as Lagrangian  $G(r)$ , Laplacian electron density  $P(r)$ , Potential energy density  $V(r)$ , Lagrangian kinetic energy  $G(r)$ , electron delocalization function (ELF), Eigen values of Hessian matrix ( $\lambda_1$ ,  $\lambda_2$ , and  $\lambda_3$ ), and the ellipticity of the bond ( $\epsilon$ ) [26]. The values of these parameters provide insights into the intensity and nature of interactions between molecules. For instance,

higher electron density  $\rho(r)$  signifies strong covalent bonds, while lower values indicate weak covalent bonds or non-covalent interactions. Laplacian electron density  $\nabla^2\rho(r)$  and Eigen values of the Hessian matrix reveal electron delocalization and the curvature of the bond critical points, respectively. Positive values of Laplacian electron density and total electron density indicate closed-shell interactions or non-covalent bonds, while negative values suggest the presence of polar covalent bonds or strong covalent interactions. Furthermore, the Langrangian kinetic energy  $G(r)$  and potential energy density  $V(r)$  offer valuable information on the kinetic motion and potential energy of the molecules, aiding in understanding their stability and reactivity. The ellipticity value ( $\epsilon$ ) serves as an indicator of structural stability, with higher values suggesting stability and lower values indicating instability. In Table 1, the topological parameters for each compound under study are presented, highlighting the characteristics of their bond critical points and the nature of chemical bonding within the

molecules [27]. The electron density distribution and electron delocalization function further confirm the degree of localization of electron density around the bonds, with values ranging from 0.000 to 1.000 indicating high electron delocalization. By correlating these detailed topological analyses with the aim of the study focused on identifying and characterizing bioactive compounds in the ethyl-acetate fraction of *H. verticillata* leaf extract for their anti-diabetic activity, researchers can gain a deeper understanding of the molecular properties and interactions that underlie the potential therapeutic effects of these compounds. This approach offers a comprehensive view of the structural features and bonding patterns that may contribute to the observed pharmacological activities related to managing diabetes. As shown in plate 4 and Table 2, the analysis of bond critical points and related properties along O13-C12, C2-C8, and C5-C11 bonds for 2-amino-1-phenylethanol reveals specific electronic characteristics and bonding interactions within the molecule, indicating its structural stability and reactivity. The Laplacian of electron density  $\nabla^2\rho(r)$  of the surfaces upon intra-atomic interaction, elucidates that the chemical bond formed between residual atoms of the systems as shown in plate 5

exhibited partial covalent interaction (shared) and more electrostatic interaction, since the Laplacian of electron density  $\nabla^2\rho(r) < 0$  and total energy density  $H(r) < 0$ ,  $G(r)/V(r) < 0.5$ . Similarly, the examination of Naphthalene and Benzoic Acid compounds provides detailed information regarding the electron density, kinetic and potential energy densities, and other essential parameters, which elucidate the molecular properties contributing to their stability and potential bioactivity. Contrastingly, 2-chloropropionic acid exhibits distinct electronic properties, as indicated by the values along the C4-C1, C2-H8, and H10-C2 bonds, reflecting differences in bonding interactions and stability compared to the other compounds studied. In the case of 1,4-Eicosadiene, the analysis of properties along various bonds such as H7-C12, H2-C5, and C6-H15 highlights specific electronic features that contribute to its structural characteristics and potential bioactive properties. The bond ellipticity (E) values of the studied bioactive compounds suggest that there is a likelihood of the chemical bonds formation between the bond critical points (BCP) of interest, to be less stable, since when  $E < 1$ , it depicts high level of stability of the bioactive systems respectively.

Table 2: The theoretically computed topological parameters (in a.u), Electron density  $\rho(r)$ , Laplacian electron density  $\nabla^2(r)$ , Lagrangian kinetic energy  $G(r)$ , Potential electron energy density  $V(r)$ , Total electron energy density  $H(r)$ , Ellipticity of bond ( $\epsilon$ ) of the studied complexes at the bond critical points (BCPs).

Bioactive compounds	Bond	BCP	$\rho(r)$	$\nabla^2\rho(r)$	$G(r)$	$K(r)$	$V(r)$	$H(r)$	$\epsilon$	EFL
2-amino-1-phenylethanol	O13-C12	20	-0.111	-0.012	0.481	0.478	-0.473	-0.478	0.360	0.842
	C2-C8	13	-0.739	-0.546	0.419	0.184	-0.184	-0.184	0.937	0.765
	C5-C11	17	-0.734	-0.538	0.477	0.184	-0.184	-0.186	0.348	0.759
Naphthalene	H37-C64	21	-0.824	-0.678	0.324	0.238	-0.270	-0.238	0.269	0.976

	C4 - C8	23	-0.830	-0.688	0.975	0.305	-0.402	-0.305	0.288	0.931
	C5-C9	25	-0.935	-0.874	0.120	0.354	-0.475	-0.354	0.315	0.923
<b>Benzoic Acid</b>	H7-C1	16	-0.925	-0.856	0.324	0.238	-0.271	-0.238	0.270	0.990
	H8 – C2	21	-0.826	-0.682	0.321	0.238	-0.270	-0.238	-0.269	0.909
	C4 – H10	11	-0.734	-0.538	0.414	0.184	0.184	-0.184	0.937	0.999
<b>2-chloropropionic acid</b>	C4 - C1	13	-0.190	-0.036	0.716	0.119	0.190	-0.119	0.179	0.840
	C2- H8	17	-0.764	-0.583	0.386	0.229	0.268	0.229	0.262	0.984
	H10- C2	18	0.769	0.591	0.386	0.229	-0.268	0.229	0.282	0.984
<b>1,4-Eicosadiene</b>	H7-C12	14	-0.625	-0.390	0.324	0.118	-0.234	-0.238	0.230	0.790
	H2 – C5	13	-0.811	-0.657	0.111	0.284	-0.220	-0.238	-0.291	0.988
	C6 – H15	17	-0.854	-0.729	0.444	0.166	0.154	-0.184	0.939	0.874

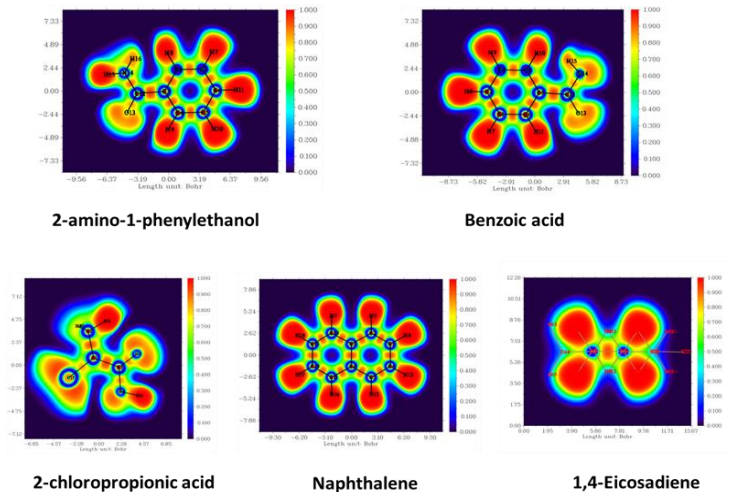


Plate 4. Electron delocalization function of the studied compounds

### 3.4.3 Molecular Electrostatic Potential (MESP)

The electrostatic potential maps are theoretical three-dimensional electron density models which depict charge distribution in a molecule with zones corresponding to reduced or increased potential energy in a molecule [28]. It generates detailed information relating to the polarity and chemical reactivity of a molecule. Electron density distribution across different regions of a molecule

indicates electrophilic and nucleophilic sites which yields information on the interaction of the molecule with the target proteins. Regions reflecting high electron density are associated with low values of electrostatic potential while high values of electrostatic potential indicate complete absence of electrons. [29] The electrostatic potential maps are valuable tool for identifying potential sites susceptible to possible electrophilic and nucleophilic attacks. The different colour scales comprise of various

hues ranging from red, yellow, blue and orange with accompanying significance.

The regions mapped in blue represent zones with positive electrostatic potential typically associated with excess electron while the red zones possess. The ESP on Benzoic acid

shows red zones explicited on the oxygen atom of the carboxylic acid group and the blue zone which indicates high electron density and possible sites of nucleophilic attack are delocalized on hydrogen atom of the carboxylic group.

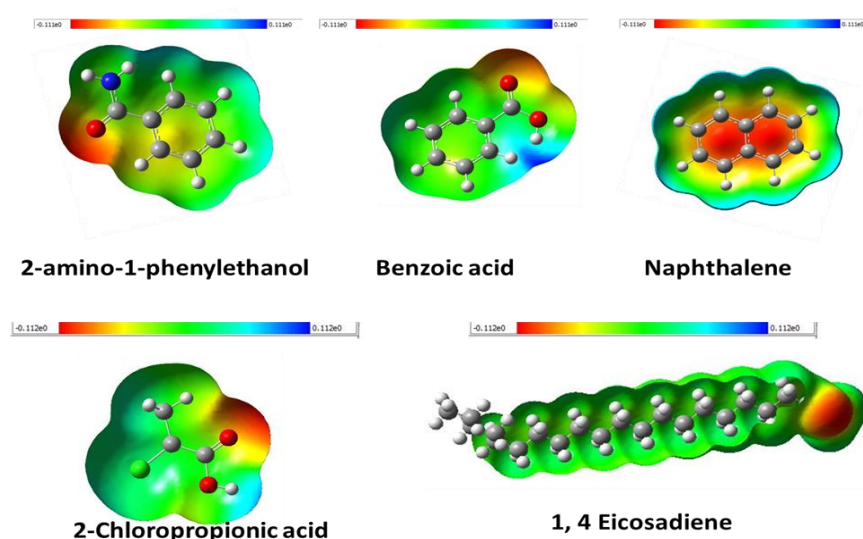


Plate 5: Molecular electrostatic potential of the studied compounds

### 3.5 Insilico-Pharmacokinetics and Toxicity Analysis

The ADME/Tox (Absorption, Distribution, Metabolism Excretion and Toxicity) studies of the compounds extract from the ethyl-hexane portion of the *H. verticillata* leaf extract was investigated by employing two web servers; SwissADME (<http://www.swissadme.ch>) [30] and ProTOX-II pharmacokinetic web servers for the validation of the oral bioavailability and toxicity respectively. The SwissADME is a unique and suitably web tool targeted at the improvement of computer aided drug design (CADD) which is a machine learning technology. The adoption of ADME in the explorative stage of drug design decreases the chances of pharmacokinetic failure in clinical phases. ProTOX-II is an online computational toxicity prediction webserver for predicting in-silico toxicity in molecules.

These web servers are freely accessible computational methods and are valid alternatives to experiments. The compounds obtained from the ethyl acetate portion of the leaf extracts were investigated for its pharmacokinetics and druglikeness using SwissADME an online Admet prediction tool. The ADMET (absorption, distribution, metabolism, excretion and toxicity) properties of the phytochemicals extracted from *Hyptis verticillata* leaf were investigated using SwissADME. While the toxicity studies were predicted using ProTox-II web server. The results of the investigated pharmacokinetic properties and druglikeness of the phytochemicals are presented in table 3. The ADMET properties were evaluated based on the Lipinski's rule of 5(RO5), which helps to predict the chemical and physical properties and the drug likeness of the phytochemicals derived from the leaf

extract. A drug is said to be active if it does not violate more than one of the rules. If a drug violates two or more of these rules it is said

to possess poor absorption [30].

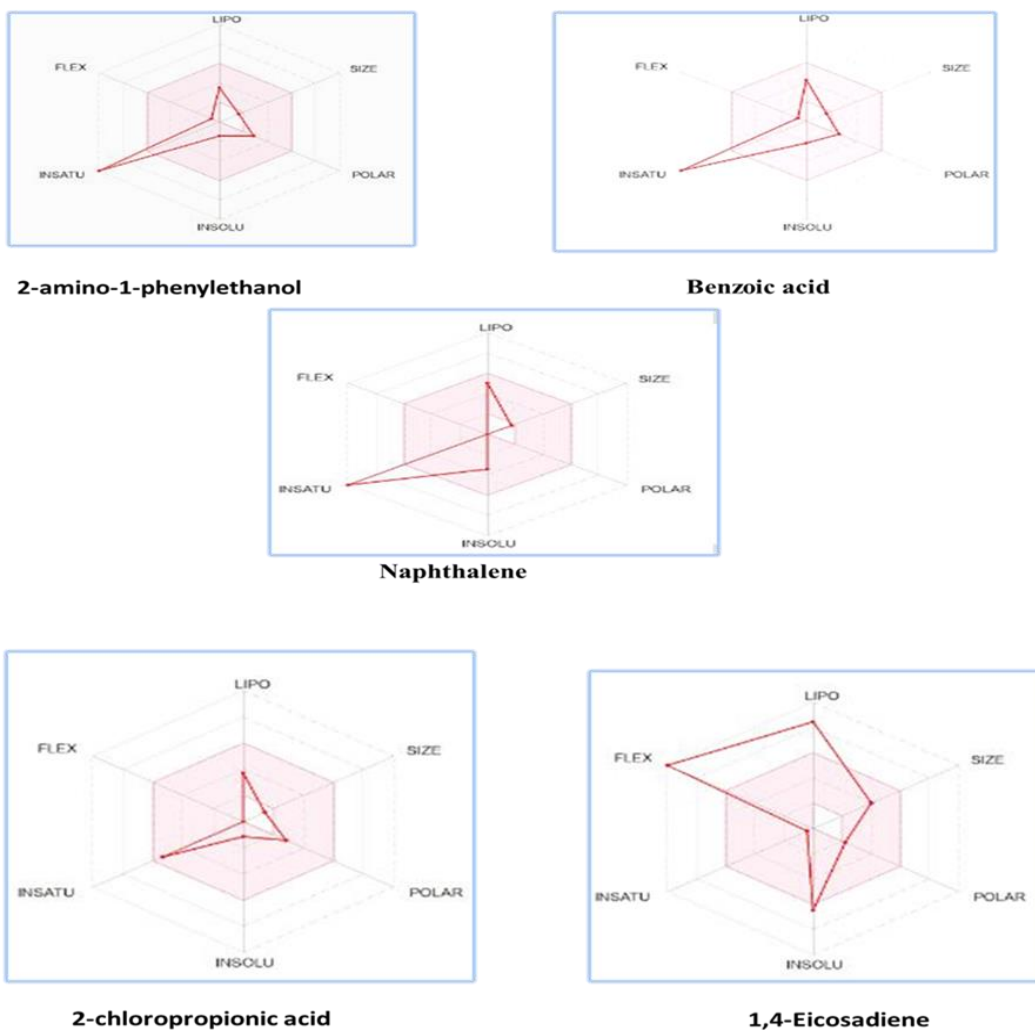


Plate 6: Bioavailability radar for the selected bioactive compounds. The Pink area represents the most desirable zone for each bioavailability parameter. LIPO = Lipophilicity, POLAR = Polarity, INSOLU = Insolubility, FLEX = Flexibility, SIZE = Molecular weight, INSATU = Unsaturation.

Table 3: Pharmacokinetics and drug likeness potentials of bioactive compounds derived from ethyl acetate fraction of *H. verticillata* leaf extract

Parameters	Benzoic acid	Naphthalene	2-amino-1-phenylethanol	2-chloropropionic acid
<b>Distribution</b>				
p-gp substrate	No	No	No	No
<b>LogK<sub>p</sub>(Skin permeation)</b>				
	-5.72cm/s	-4.7cm/s	-6.58cm/s	-6.5cm/s
BBB permeant	Yes	Yes	Yes	Yes
<b>Pharmokinetics/Metabolism</b>				
GI absorption	High	Low	High	High
CYP1A2 inhibitor	No	No	No	No
CYP2C19 inhibitor	No	No	No	No
CYP2C9 inhibitor	No	No	No	No
CYP2D6 inhibitor	No	No	No	No
<b>Druglikeness</b>				
Lipinski	Yes; 0 violation	Yes; 0 Violation	Yes; 0 violation	Yes; 0 violation
Ghose	No; 0 violations:	No; 1 violations	No; 0 violations:	No; 0 violations:
Bioavailability Score	0.85	0.55	0.55	0.85
Egan	Yes	Yes	Yes	Yes
Veber	Yes	Yes	Yes	Yes
<b>Water solubility</b>				
Log S (ESOL)	-2.20	-3.45	-4.21	-5.34
Solubility	7.66e-01mg/ml; 01mg/ml;	1.36e-01mg/ml; 9.227e-05mol/l	4.59e+00mg/ml ; 3.7e-02mol/l	3.42+00mg/ml; 3.18e-02 mol/l

### 3.5.1 Distribution

The P-glycoprotein plays a crucial role in the excretion process also participates actively playing a crucial role in active efflux across biological membranes by pumping out drugs, toxins and other substances out of the liver and kidney into urine and bile respectively. Thus, reducing their accumulation in the blood stream. It is a transporter protein found

mostly in the tissues of the intestines, and in other vital organs such as the kidney and liver. The compounds under investigation were not P-glycoprotein substrates indicating their limitless access to its absorption and bioavailability [31]. The ability of a potential drug to be absorbed by the skin can be evaluated using the LogK<sub>p</sub>. By implication, negative LogK<sub>p</sub> values

indicate solubility in aqueous phase such as water. Conversely, positive values indicate the compounds preference for the octanol solvent. The compounds exhibited negative LogK<sub>p</sub> values for all the studied compounds, indicating its poor skin penetrating ability. The blood-brain barrier (BBB) permeation predicted by utilizing the BOILED-egg model, typically measures the tendency of the compound to cross the blood brain barrier to the brain. Positive values of BBB permeability indicate its tendency to cross the blood brain barrier.

### 3.5.2 Pharmacokinetics

Gastrointestinal absorption is a vital prerequisite for assessing the capability of a phytochemical to be absorbed from the gastro-intestinal tract into the blood stream. High values of GI absorption indicate the compounds' ability to be easily absorbed by the gastro-intestinal tract resulting in a cell membrane permeability and good oral bioavailability [32]. However, the compounds benzoic acid 2-amino and 2-chloropropionic acid and 1,4-Eicosadiene exhibited high GI absorption predictions. The 5 compounds do not inhibit the CYP1A2, CYP2C19, CYP2C9 and CYP2D6 enzymes indicating that it may not be metabolized by these enzymes. Resulting in little or no possibility of their interference with the metabolism of other drugs that are metabolized by these enzymes.

### 3.5.3 Water solubility

Solubility is one major factor influencing drug absorption for orally administered drug. It significantly affects its rate of absorption in the body. For injectables, high solubility in water is required to deliver an adequate amount of active ingredient in a minute

volume contained in a dosage [33]. The five compounds with negative Log S (Ali) partition co-efficient were found to be more soluble in water than in other non-polar solvents indicating improved pharmacokinetic properties. The five compounds were soluble in water. It is worthy of note that compounds with good water solubility and high-water solubility generally are more likely to have better pharmacokinetic properties as well as improved chances of success in the drug development process.

### 3.5.4 Drug likeness

Drug likeness is the quantitative assessment of the potential of a molecule to be considered due to its suitability to be orally administered as a drug considering its bioavailability. The compounds obeyed the Lipinski rule having weight < 500 Da (g/mol), LogP ≤ 5, hydrogen bond donors ≤ 5 and hydrogen bond acceptors ≤ 10 with the exception of Naphthalene showing one violation. Naphthalene violated the Ghose rule indicating poor oral availability. The Vegan rule [40] for compounds having <10 rotatable bonds and the Egan rule indicating high solubility of the compounds were adhered to by the compounds, increasing their chance of being used as a clinical drug.

### 3.5.5 Toxicity

The toxicity studies assess the values of the various parameters utilized to interpretate toxicity scores which indicates the magnitude of apprehension associated with the toxicity level of a potential drug. As observed in table 3 all the compounds displayed little or no side effect in the light of the prediction models used in the investigation. The compounds were considered to possess excellent

pharmacokinetic properties as there was a better toxicity outcome in the retrieved toxicity results. The investigated compounds were non-carcinogenic as they were considered as inactive carcinogenic agents. They were negative to immunotoxicity by implication it has no adverse effect on the immune system [41]. Four of the compounds were non-hepatotoxic, they have no ability to cause long or short-term damage to any vital organ including the liver and kidney except for 1, 4-Eicosadiene which showed hepatotoxicity. They were also regarded as non-mutagenic, non-cytotoxic.

### 3.6 In-silico molecular docking

#### 3.6.1 Protein Preparation and Molecular Docking Protocol

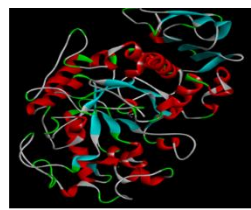
Molecular docking is an essential computational tool employed by scientist in modern in-silico drug design and possible exploration and discovery of novel chemotherapeutic compounds with suitability for use as potential drug

It has been documented as one of the most accurate and cost-effective computer assisted drug design used both in the academic and industrial sector. This bio-informatics modelling technique involves the ligand and receptor protein interaction. Facilitated by intermolecular interactions such as Vander Waal forces, electrostatic forces and hydrogen bonding. The receptor for alpha amylase and alpha glucosidase respectively (PDB ID: 2VQ4 and 7KBR) proteins were downloaded from Protein data bank database ([www.RSCPDB.org](http://www.RSCPDB.org)). while the standard drugs Acarbose and Miglitol were downloaded from drug data bank. The preparation of the receptor proteins was done using Biovia Discovery Studio 2021 Client [34] wherein water molecules, native ligands were deleted and polar hydrogens were added to enhance binding compatibility. These

prepared proteins were saved in PDB format. The prepared target proteins were loaded in PyRx [35] virtual screening tool as a starting protein in Pdbqt format. The target proteins were transformed into macromolecules using Auto dock, which resulted in the atomic coordinates being converted to pdbqt format. The compounds were selected, subjected to energy minimized and converted to pdbqt format using Open Babel.

A grid box showed at the centre of the target sites with dimensions set at 25x 25x25Å using an exhaustiveness value of 8. The actual docking of the receptor protein and the ligand was conducted using autodock vina embedded in PyRx. The docking scores were generated with the best poses and the exported files were saved as PyRx\_Autodock4.tar c. Both the prepared protein in PDB format and the Ligand poses in pdbqt format from the same folder were dragged and dropped into the Biovia Discovery Studio. The define receptor/define ligand tab was employed to specify the receptor and ligand, and the step through ligand feature was employed to show the various ligand-protein interactions. 2D visualization showcased the interactions with the ligands and protein amino acid residues. To ascertain the best Ligand-protein interaction, the amount of hydrogen bonds and binding affinity were noted as well as the bond lengths of the ligands and the residual amino acids. For 3D visualization, PyMol Stereo 3D Zalman software was employed. First the prepared protein in pdbqt was dragged in the Pymol interface, so was also the best pose as obtained from the 2D visualization done in Biovia discovery studio. The protein and ligand sites were preset to Cartoon mode, after which the amino acid residues was labelled via polar

contacts. These views enabled us obtain details of the protein-ligand interactions.



Alpha Amylase (PDB ID: 2QV4)



Alpha Glucosidase (PDB ID: 7KBR)

Plate 7: The receptor proteins downloaded from protein data bank

Molecular docking primarily focuses on binding poses and binding affinity predictions. Accurate predictions of binding poses and binding affinities have the potential to reduce costly experimental efforts while also identifying promising drug candidates. The strength and stability of the protein-ligand interaction are indicated by the negative sign of binding affinities in molecular docking. The more negative the binding affinity the stronger the bonds between the protein and the ligands [36]. Increased negativity of the electron affinity indicates greater stability of the interactions between the ligand and the protein.

The thermodynamic equation  $\Delta G = \Delta H - T\Delta S$ , where  $\Delta G$  is the Gibbs free energy,  $\Delta H$  is the enthalpy change,  $T$  is the absolute temperature, and  $S$  is the entropy change, is what gives binding affinities their negative sign. The  $\Delta G$  in molecular docking represents the protein and ligands binding affinity. The fact that the binding affinity is negative suggests that the interaction is predominantly driven by the enthalpy change ( $\Delta H$ ) as it is typically negative for protein-ligand interactions. In analysing interactions

between receptor proteins and ligands in biological systems, hydrogen bonds are frequently the most prevalent type of interaction used as a measure of interactive strength [37]. The strength and stability of the protein-ligand interaction are further determined by the length of the hydrogen bond between the protein and the ligand. The shorter the bond length, the longer the connection that exists between the protein and the ligand. Hydrogen bonds are typically the most predominant bonds in Protein-ligand interactions in biological systems. However, the bond length of the hydrogen bond between the protein and the ligand is important to ascertain the strength and stability of the protein-ligand interaction wherein, the shorter the bond length, the longer the interaction between the protein and the ligand. The presence of high binding affinities and significant conventional hydrogen interaction is a great indicator for determining effective interaction.

The docking analysis of Alpha Amylase (PDB ID: 2QV4) and the compounds obtained from *H. verticillata* leaf extract showed promising anti-diabetic properties as

they exhibited better binding affinities at the correct binding sites. The molecular docking of alpha-amylase with the obtained compounds; 2-amino-1-phenylethanol, benzoic acid, 2-chloropropionic acid, naphthalene and 1,4 Eicosadiene, generated different values of binding affinities with the highest value deemed as the best pose in the order of -5.7kcal/mol, -5.6 kcal/mol, -5.5kcal/mol, 5.9kcal/mol and -6.0 kcal/mol. Although the standard drugs utilized in this investigation were Miglitol and Acarbose. Docking results of binding interactions between alpha amylase and Miglitol showed the binding affinity of -5.5 kcal/mol, formed three conventional hydrogen bonds HIS:299, ASP:300 GLU: 233. The bond lengths for these interactions were measured at 2.48Å, 2.61Å, 2.02Å, respectively with no accompanying amino acid residue while Acarbose showed a binding affinity of 7.0kcal/mol as the best pose. Showing different interactions and residues with hydrogen bonds being the most predominant at different bond lengths HIS: 305 (2.21 Å), ASP: 300 (1.45Å) GLU: 233 (2.65 Å) and Pi-Pi Stacked TYR: 62 (4.22 Å). The compounds showed more efficacy in the increasing trend 1, 4Eicosadiene > naphthalene> 2-amino-1-phenylethanol > benzoic acid >2 -chloropropionic acid in terms of their increasing binding affinity. Indicating their efficacy in the inhibition of its target receptor. In comparison to the standard drug, the compounds exhibited greater inhibition than compared to miglitol. Although Acarbose had a higher inhibition on alpha amylase than the compounds and miglitol.

The results of the best conformation with the associated interacting amino acids residues,

binding affinity and the binding distances of the interaction between the compounds and  $\alpha$ -glucosidase is presented in table 4. From the obtained docking results the binding interactions of  $\alpha$ -glucosidase (PDB ID: 7KBR) and the compounds showed conventional hydrogen and other residues. 2-aminophenylethanol had a binding affinity of -4.6kcal/mol with two conventional hydrogen bonds ARG A: 195 (2.45) HIS A: 299(2.65), Pi-donor hydrogen bond TYR A: 62(2.98).

Benzoic acid possessing binding affinity of -4.7kcal/mol with hydrogen bond HIS A: 299 (2.65), Pi-Pi Stacked TYR A: 62(4.54) interactions. Naphthalene showed the binding affinity of -5.1kcal/mol accompanied by Pi-Pi Stacked TRP:J:344, Pi-Alkyl ARG J:300, PRO J:314 and ARG I:35 as residue. 2-chloro-1-phenylethanol had the binding affinity of 4.8kcal/mol with Pi-Sigma TRP A: 709 as residue. Miglitol with the binding affinity of -4.6kcal/mol showed five conventional hydrogen bonds ASP: 849 (2.45Å), ASP : 54 (2.10 Å), TYR : 106 (2.40 Å), TRP : 910 (2.51Å), VAL : 92 (2.13 Å) . Docking of Acarbose with showed four conventional hydrogen bonds with the binding affinity of -6.0Kcal/mol. The compounds exhibited good compatibility with  $\alpha$ -amylase and  $\alpha$ -glucosidase thereby generated high binding affinities with lesser number of hydrogen bonds. According to the principles outlined in the Lipinski rule of five, which suggests that compounds with more than five hydrogen-bond acceptors tend to exhibit limited absorption or penetration properties. In the case, compounds were found to be more potent than Miglitol used the standard drug used, but less potent than Acarbose.

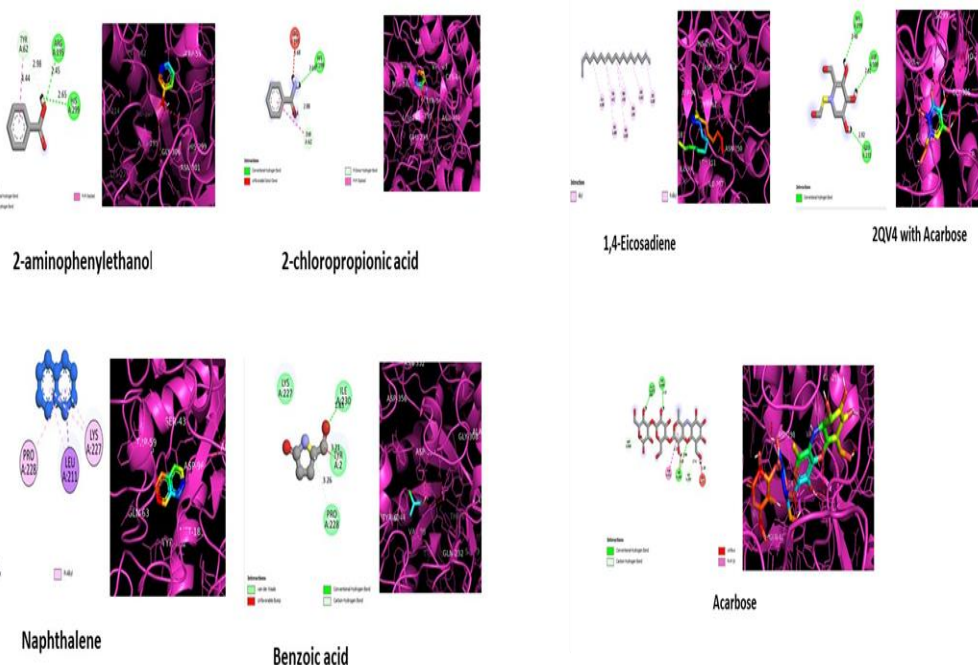


Plate 8:2D and 3D visualization of molecular docking of Alpha Amylase (2QV4) with the ligands and standard drugs

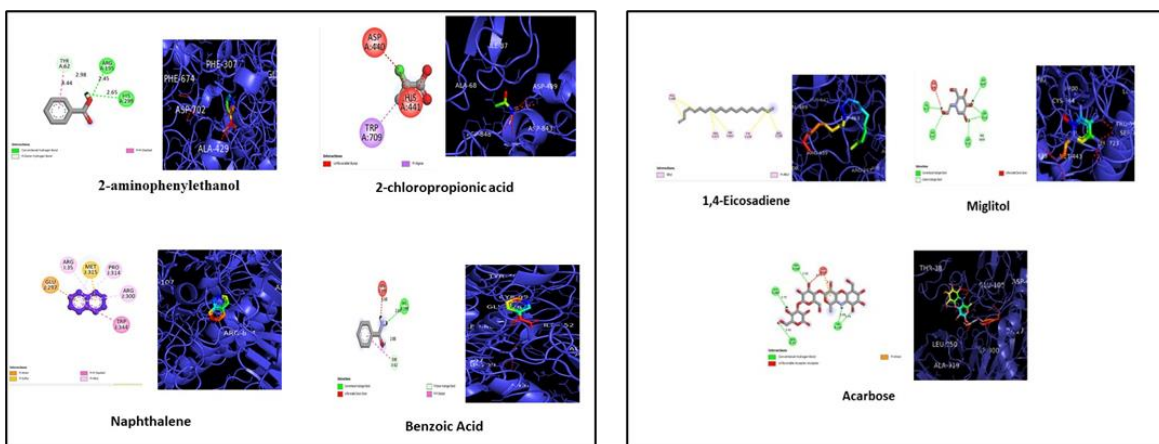


Plate 9: 2D and 3D visualization of molecular docking of Alpha Glucosidase (7KBR) with the ligands and standard drugs

## 4.0 Conclusion

This study aimed to elucidate and characterize the bioactive constituents present in the ethyl-acetate fraction of *H. verticillata* Jacq leaf extract, attributing to its

anti-diabetic activity. Utilizing Gas Chromatography-Mass Spectrometry (GC-MS) analysis, the active compounds in the plant extract were identified, providing crucial idea into the chemical constituents

responsible for the observed anti-diabetic efficacy. This exploration substantiated the traditional utilization of *H. verticillata* Jacq leaf in indigenous medicinal practices, particularly in the management of diabetes. Further exploration delved into the molecular attributes of the identified compounds through theoretical scrutiny of frontier molecular orbitals and quantum descriptors. The electrophilicity index was instrumental in understanding the chemical reactivity of these compounds within biological milieu, while the ionization potential values offered indications of the stability exhibited by the phytochemical entities derived from the ethyl-acetate fractions of the plant extract. The density of states analysis accentuated the significant involvement of carbon and hydrogen moieties within the energy level spectrum of 0.7 - 0.2 atomic units, indicative of augmented compound stability. Moreover, the Natural Bond Orbital (NBO) analysis unveiled high stabilization energy, suggestive of potential intermolecular interactions between donor and acceptor orbitals of the compounds. Non-covalent interactions (NCI) evaluations endorsed the presence of diverse intra and intermolecular attractive forces, highlighting the non-covalent nature of the compounds. The observation of green spikes across the ethyl-acetate fractions speaks of the predominance of van der Waals forces, enhancing the operational efficacy of the compounds as pharmacological agents.

In addition, molecular docking simulations, a computational drug design strategy, showcased the superior inhibitory capacity of the phytochemical constituents within the ethyl-acetate fractions of *H. verticillata* Jacq leaf extract in comparison to miglitol, a benchmark diabetic drug. Assessment of Absorption, Distribution, Metabolism,

Excretion, and Toxicity (ADMET) profiles elucidated the pharmaceutical attributes of the extracted compounds, with notable candidates such as benzoic acid 2-amino, 2-chloropropionic acid, and 1,4-Eicosadiene exhibiting favourable gastrointestinal absorption predictions, commendable oral bioavailability, negligible cytotoxicity, and enhanced anti-diabetic properties. These findings suggest the safety profile, aqueous solubility, and promising pharmaceutical utility of these compounds in the efficacious management of diabetes.

## 5.0 Declarations

### 5.1 Acknowledgements.

We appreciate the centre for high-performance computing (CHPC), South Africa for providing the computational resources needed to actualize this research

### 5.2 Declaration of Competing Interest

All authors declare zero financial or interpersonal conflict of interest that could have influenced the research work

### 5.3 Funding

This research was not funded by any Governmental or Non-governmental agency.

### 5.4 Authors' contributions

Egbung, Godwin Eneji: Project conceptualization, design, and supervision. Ukam, Catherine Ironya-Ogar and Ogar, Blessing Thomas: Writing, results extraction, analysis, and manuscript first draft: Chume, Sandra and Abuo Patrick: Manuscript writing, review, analysis, and proofreading. Ibiam Okoro and Ekom Monday: Manuscript Proofreading. Atangwho, Item Justin; Egbung, Josephine Eneji and Edet, Henry Okon: Resources, review, and editing.

## References

Zhou, B., Carrillo-Larco, R. M., Danaei, G., Riley, L. M., Paciorek, C. J., Stevens,

G. A., & Breckenkamp, J. (2021). Worldwide trends in hypertension prevalence and progress in treatment and control from 1990 to 2019: a pooled analysis of 1201 population-representative studies with 104 million participants. *The Lancet*, 398(10304), 957-980.

Li, Y., Wang, J., Xu, Y., Meng, Q., Wu, M., Su, Y., & Wang, Y. (2023). The water extract of *Potentilla discolor* Bunge (PDW) ameliorates high-sugar diet-induced type II diabetes model in *Drosophila melanogaster* via JAK/STAT signalling. *Journal of Ethnopharmacology*, 116760.

Parveen, A., Jin, M., & Kim, S. Y. (2018). Bioactive phytochemicals that regulate the cellular processes involved in diabetic nephropathy. *Phytomedicine*, 39, 146-159.

Edet, H. O., Louis, H., Godwin, U. C., Adalikwu, S. A., Agwamba, E. C., & Adeyinka, A. S. (2023). Single-metal (Cu, Ag, Au) encapsulated gallium nitride nanotube (GaNNT) as glucose nonenzymatic nanosensors for monitoring diabetes: Perspective from DFT, visual study, and MD simulation. *Journal of Molecular Liquids*, 122209.

Ogar, I., Egbung, G.E., Nna, V. D., Iwara, I. A. and Itam, E. (2018). Anti-hyperglycaemic potential of *Hyptis verticillata* jacq in streptozotocin-induced diabetic rats. *Biomedicine & Pharmacotherapy*, 107: 1268 – 1276.

DiSpirito, J. R., & Mathis, D. (2015, September). Immunological contributions to adipose tissue homeostasis. In *Seminars in immunology* (Vol. 27, No. 5, pp. 315-321). Academic Press.

Saeedi, P., Petersohn, I., Salpea, P., Malanda, B., Karuranga, S., Unwin, N. & IDF Diabetes Atlas Committee. (2019). Global and regional diabetes prevalence estimates for 2019 and projections for 2030 and 2045: Results from the International Diabetes Federation Diabetes Atlas. *Diabetes research and clinical practice*, 157, 10784.

Sharma, P., Joshi, T., Joshi, T., Chandra, S., & Tamta, S. (2020). In silico screening of potential antidiabetic phytochemicals from *Phyllanthus emblica* against therapeutic targets of type 2 diabetes. *Journal of ethnopharmacology*, 248, 112268.

Picking, D., Chambers, B., Barker, J., Shah, I., Porter, R., Naughton, D. P., & Delgoda, R. (2018). Inhibition of cytochrome P450 activities by extracts of *Hyptis verticillata* Jacq.: Assessment for potential HERB-drug interactions. *Molecules*, 23(2), 430.

Mérial-Mamert, V., Ponce-Mora, A., Sylvestre, M., Lawrence, G., Bejarano, E., & Cebrián-Torrejón, G. (2022). Antidiabetic potential of plants from the Caribbean basin. *Plants*, 11(10), 1360.

Lianza, M., Poli, F., Nascimento, A. M. D., Soares da Silva, A., da Fonseca, T. S.,

Toledo, M. V., ... & Leitão, S. G. (2022). In vitro  $\alpha$ -glucosidase inhibition by Brazilian medicinal plant extracts characterised by ultra-high performance liquid chromatography coupled to mass spectrometry. *Journal of Enzyme Inhibition and Medicinal Chemistry*, 37(1), 554-562.

Atangwho, I. J., Egbung, G. E., Ahmad, M., Yam, M. F., & Asmawi, M. Z. (2013). Antioxidant versus anti-diabetic properties of leaves from *Vernonia amygdalina* Del. growing in Malaysia. *Food chemistry*, 141(4), 3428-3434.

Louis, H., Patrick, M., Amodu, I. O., Benjamin, I., Ikot, I. J., Iniama, G. E., & Adeyinka, A. S. (2023). Sensor behavior of transition-metals (X= Ag, Au, Pd, and Pt) doped Zn11-X-O12 nanostructured materials for the detection of serotonin. *Materials Today Communications*, 34, 105048.

Asogwa, F. C., Apebende, C. G., Ugodi, G. W., Ebo, P., Louis, H., Ikeuba, A. I., ... & Owen, A. E. (2022). Anti-inflammatory, Immunomodulatory and DFT Evaluation of the Reactivity Indexes of Phytochemicals Isolated from *Harungana madagascariensis*. *Chemistry Africa*, 1-13.

Ogar, I., Egbung, G. E., Nna, V. U., Atangwho, I. J., & Itam, E. H. (2019). *Hyptis verticillata* attenuates dyslipidaemia, oxidative stress and hepato-renal damage in streptozotocin-induced diabetic rats. *Life sciences*, 219, 283-293.

El Aissouq, A., Bouachrine, M., Ouammou, A., & Khalil, F. (2022). Homology modelling, virtual screening, molecular docking, molecular dynamic (MD) simulation, and ADMET approaches for identification of natural anti-Parkinson agents targeting MAO-B protein. *Neuroscience Letters*, 786, 136803.

Asogwa, F. C., Agwamba, E. C., Louis, H., Muozie, M. C., Benjamin, I., Gber, T. E., & Ikeuba, A. I. (2022). Structural benchmarking, density functional theory simulation, spectroscopic investigation and molecular docking of N-(1H-pyrrol-2-yl) methylene)-4-methylaniline as castration-resistant prostate cancer chemotherapeutic agent. *Chemical Physics Impact*, 5, 100091.

Harbone, J. B., (1973). *Text Book of Phytochemical Methods*, 1st edition. Champraan and hall limited, London, UK., 110-113

Sengupta, A., Li, B., Svatunek, D., Liu, F., & Houk, K. N. (2022). Cycloaddition reactivities analysed by energy decomposition analyses and the frontier molecular orbital model. *Accounts of Chemical Research*, 55(17), 2467-2479.

Koopmans, T. C. (1960). Stationary ordinal utility and impatience. *Econometrica: Journal of the Econometric Society*, 287-309.

Weinhold, F., Landis, C. R., & Glendening, E. D. (2016). What is NBO analysis and how is it useful? *International reviews in physical chemistry*, 35(3), 399-440.

Ibrahim, M., Abbad, M., & Khaild, M. (2018). Phytochemical, crystal structure, spectroscopic, DFT based

noncovalent interactions and non-linear optical studies of *Neurada procumbens*. *Journal of the Chemical Society of Pakistan*, 40(4), 749-760.

Gowrishankar, S., Muthumanickam, S., Kamaladevi, A., Karthika, C., Jothi, R., Boomi, P., ... & Pandian, S. K. (2021). Promising phytochemicals of traditional Indian herbal steam inhalation therapy to combat COVID-19—An in silico study. *Food and Chemical Toxicology*, 148, 111966.

Zhu, J., Zhang, D., Tang, H., & Zhao, G. (2018). Structure relationship of non-covalent interactions between phenolic acids and arabinan-rich pectic polysaccharides from rapeseed meal. *International journal of biological macromolecules*, 120, 2597-2603.

Adalikwu, S. A., Louis, H., Iloanya, A. C., Edet, H. O., Akem, M. U., Eno, E. A., & Manicum, A. L. E. (2022). B-and Al-Doped Porous 2D Covalent Organic Frameworks as Nanocarriers for Biguanides and Metformin Drugs. *ACS Applied Bio Materials*, 5(12), 5887-5900.

Rahman, M. M., Biswas, S., Islam, K. J., Paul, A. S., Mahato, S. K., Ali, M. A., & Halim, M. A. (2021). Antiviral phytochemicals as potent inhibitors against NS3 protease of dengue virus. *Computers in Biology and Medicine*, 134, 104492.

Ghalami-Choobar, B., & Moghadam, H. (2018). Molecular docking based on virtual screening, molecular dynamics and atoms in molecules studies to identify the potential human epidermal receptor 2 intracellular domain inhibitors. *Physical Chemistry Research*, 6(1), 83-103.

Raajaraman, B. R., Sheela, N. R., & Muthu, S. (2019). Spectroscopic, quantum computational and molecular docking studies on 1-phenylcyclopentane carboxylic acid. *Computational Biology and Chemistry*, 82, 44-56.

Gopinath, K., Karthikeyan, C., Hameed, A. H., Arunkumar, K., & Arumugam, A. (2015). Phytochemical synthesis and crystallization of sucrose from the extract of *Gloriosa superba*. *Research Journal of Phytochemistry*, 9(4), 144-160.

Raju, T. P., Shastri, K. J. R., Reddy, C. S., & Reddy, V. M. (2010). Antihyperglycemic activity of *Strychnos potatorum* seed and leaf methanolic extracts in alloxan-induced diabetic rats. *Research Journal Of Pharmacognosy and Phytochemistry*, 2(2), 152-154.

Idante, P. S., Apebende, G. C., Louis, H., Benjamin, I., Undiandeye, U. J., & Ikot, I. J. (2023). Spectroscopic, DFT study, and molecular docking investigation of N-(3-methylcyclohexyl)-2-phenylcyclopropane-1-carbohydrazide as a potential antimicrobial drug. *Journal of the Indian Chemical Society*, 100(2), 100806.

Ebong, P. E., Atangwho, I. J., Eyong, E. U., & Egbung, G. E. (2008). The

antidiabetic efficacy of combined extracts from two continental plants: *Azadirachta indica* (A. Juss) (Neem) and *Vernonia amygdalina* (Del.) (African bitter leaf). *American journal of Biochemistry and Biotechnology*, 4(3), 239-244.

Yalcin, S. (2020). Molecular Docking, Drug Likeness, and ADMET Analyses of *Passiflora* compounds as P-glycoprotein (P-gp) inhibitor for the treatment of cancer. *Current Pharmacology Reports*, 6, 429-440.

Jia, C. Y., Li, J. Y., Hao, G. F., & Yang, G. F. (2020). A drug-likeness toolbox facilitates ADMET study in drug discovery. *Drug discovery today*, 25(1), 248-258.

Daina, A., Michielin, O., & Zoete, V. (2017). SwissADME: a free web tool to evaluate pharmacokinetics, drug-likeness and medicinal chemistry friendliness of small molecules. *Scientific reports*, 7(1), 42717.

Sajesh, B. V., On, N. H., Omar, R., Alrushaid, S., Kopec, B. M., Wang, W. G., ... & Miller, D. W. (2019). Validation of cadherin HAV6 peptide in the transient modulation of the blood-brain barrier for the treatment of brain tumors. *Pharmaceutics*, 11(9), 481.

Afahanam, L. E., Louis, H., Benjamin, I., Gber, T. E., Ikot, I. J., & Manicum, A. L. E. (2023). Heteroatom (B, N, P, and S)-doped cyclodextrin as a hydroxyurea (HU) drug nanocarrier: a computational approach. *ACS omega*, 8(11), 9861-9872.

Wei, K., Louis, H., Emori, W., Idante, P. S., Agwamba, E. C., Cheng, C. R., Eno, E. A. & Unimuke, T. O. (2022) Antispasmodic Activity of Carnosic Acid Extracted from *Rosmarinus Officinalis*: Isolation, Spectroscopic Characterization, DFT Studies, and in Silico Molecular Docking Investigations. *Journal of Molecular Structure*, 132795. <https://doi.org/10.1016/j.molstruc.2022.132795>.

Utsu, P. M., Gber, T. E., Nwosa, D. O., Nwagu, A. D., Benjamin, I., Ikot, I. J., & Louis, H. (2023). Modeling of Anthranilhydrazide (HL1) Salicylhydrazone and Its Copper Complexes Cu (I) and Cu (II) as a Potential Antimicrobial and Antituberculosis Therapeutic Candidate. *Polycyclic Aromatic Compounds*, 1-19.